

# A piecewise linear transverse shear transfer model for bolted side-plated beams

Ling-Zhi Li<sup>1a</sup>, Chang-Jiu Jiang<sup>\*1</sup>, Ray Kai-Leung Su<sup>2b</sup> and Sai-Huen Lo<sup>2c</sup>

<sup>1</sup>Research Institute of Structural Engineering and Disaster Reduction, College of Civil Engineering, Tongji University, 1239 Siping Road, Shanghai 200092, China

<sup>2</sup>Department of Civil Engineering, The University of Hong Kong, Pokfulam Road, Hong Kong

(Received April 21, 2015, Revised February 20, 2017, Accepted March 9, 2017)

**Abstract.** The performance of bolted side-plated (BSP) beams is affected by the degree of transverse partial interaction, which is a result of the interfacial slip caused by transverse shear transfer between the bolted steel plates and the reinforced concrete beams. However, explicit formulae for the transverse shear transfer profile have yet to be derived. In this paper, a simplified piecewise linear shear transfer model was proposed based on force superposition principle and simplification of shear transfer profiles derived from a previous numerical study. The magnitude of shear transfer was determined by force equilibrium and displacement compatibility condition. A set of design formulae for BSP beams under several basic load cases was also derived. Then the model was verified by test results. A worked example was also provided to illustrate the application of the proposed design formulae. This paper sheds some light on the shear force transfer mechanism of anchor bolts in BSP beams, and offers a practical method to evaluate the influence of transverse partial interaction in strengthening design.

**Keywords:** reinforced concrete beam; strengthening; bolted side-plated beam; curvature factor; transverse partial interaction; transverse slip; transverse shear transfer; piecewise linear

## 1. Introduction

When reinforced concrete (RC) beams are under the requirement of strengthening, providing adequate ductility and energy dissipation is essential to avoid sudden catastrophic failure. However, available retrofitting methods, such as attaching steel plates or fibre-reinforced polymers to the beam soffits by adhesive bonding, may lead to serious debonding and peeling failures, thus unable to attain the design strength (Adhikary *et al.* 2000, Ahmed *et al.* 2000, Anil *et al.* 2010). On the other hand, bolting steel plates to the side faces of RC beams by anchor bolts, i.e., the bolted side-plating (BSP) technique, suppresses these premature failures (Subedi and Baglin 1998, Su and Zhu 2005), despite the fact that the BSP beams also have some shortcomings, such as their susceptibility to plate buckling (Smith and Bradford 1999) and reduction in flexural strength due to bolt slippage (Johnson and Molenstra 1991, Oehlers *et al.* 1997, Siu and Su 2011).

Partial interaction, as a result of both the longitudinal and the transverse bolt slips (Su *et al.* 2013), caused by the

shear force transfer between the steel plates and the RC beam through the bolt connections, is one of the key parameters controlling the strengthening effect of BSP beams (Oehlers *et al.* 2000). The degree of partial interaction in the longitudinal and the transverse directions can be measured by the following two factors (Siu and Su 2010, Zhu and Su 2010)

$$\alpha_\varepsilon = \varepsilon_{p,y_{pc}} / \varepsilon_{c,y_{pc}} \quad (1)$$

$$\alpha_\varphi = \varphi_p / \varphi_c \quad (2)$$

The symbols in Eqs. (1), (2) are defined in Fig. 1, which illustrates a cross section of a BSP beam. The concrete and the steel plates are divided into  $m$  and  $n$  layers, and the reinforcements are also divided into  $s$  layers according to the actual arrangement of the rebars.  $i, j, k$  is the layer indexes of concrete, reinforcements and steel plates respectively. Accordingly,  $y_{c,i}, y_{s,k}, y_{p,j}, A_{c,i}, A_{s,k}, A_{p,j}, \varepsilon_{c,i}, \varepsilon_{s,k}, \varepsilon_{p,j}$  is the distance from the centre of the layer to the beam's bottom surface, the layer area, the strain at the center of the layer of concrete, reinforcements and steel plates, respectively.  $d_c$  and  $d_p$  is the layer thickness of concrete and steel plates, respectively.  $\alpha_\varepsilon$  is the strain factor defined as the ratio between longitudinal strains of the steel plates ( $\varepsilon_{p,y_{pc}}$ ) and the RC beam ( $\varepsilon_{c,y_{pc}}$ ) at the centroidal level of steel plates ( $y_{pc}$ ), and is used to denote the axial strain lagging of the steel plates due to the longitudinal bolt slip  $S_{lc}$ ;  $\alpha_\varphi$  is the curvature factor defined as the ratio between curvatures of the steel plates ( $\varphi_p$ ) and the RC beam ( $\varphi_c$ ), and is used to denote the curvature reduction of the steel plates

\*Corresponding author, Ph.D. Candidate

E-mail: 99jchj@tongji.edu.cn

<sup>a</sup>Assistant Professor

E-mail: lilingzhi@tongji.edu.cn

<sup>b</sup>Associate Professor,

E-mail: klsu@hku.hk

<sup>c</sup>Professor

E-mail: hreclsh@hku.hk

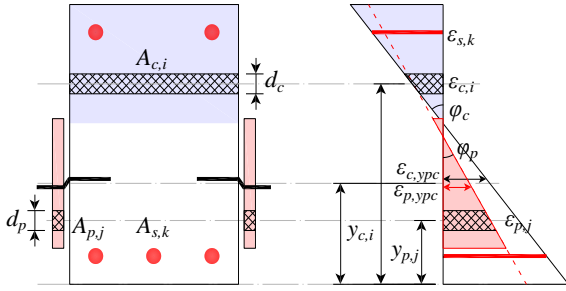


Fig. 1 Strain profiles of a BSP section with partial interaction

due to the transverse bolt slip  $S_{tr}$ .

In a moment-curvature analysis of a RC beam, the strains of concrete and reinforcement can be expressed in terms of the curvature ( $\varphi_c$ ) and the neutral axis level ( $y_{na}$ ) of the RC beam

$$\varepsilon_{c,i} = \varphi_c (y_{c,i} - y_{na}) \quad i = 1, \dots, m \quad (3)$$

$$\varepsilon_{s,k} = \varphi_c (y_{s,k} - y_{na}) \quad k = 1, \dots, s \quad (4)$$

Similarly, if the two factors ( $\alpha_\varepsilon$  and  $\alpha_\varphi$ ) in Eqs. (1)-(2) is known, the flexural strain profile of the steel plates in a BSP beam can also be expressed in term of the same two unknowns ( $\varphi_c$  and  $y_{na}$ )

$$\begin{aligned} \varepsilon_{p,j} &= \varepsilon_{p,y_{pc}} + \varphi_p (y_{p,j} - y_{pc}) \\ &= \alpha_\varepsilon \varphi_c (y_{pc} - y_{na}) + \alpha_\varphi \varphi_c (y_{p,j} - y_{pc}) \end{aligned} \quad (5)$$

$j = 1, \dots, n$

Thus the internal loading state of a BSP section under a certain bending moment  $M$  can be determined by solving the two unknowns ( $\varphi_c$  and  $y_{na}$ ) accordingly

$$\begin{aligned} \sum N &= bd_c \sum \sigma_c(\varepsilon_{c,i}) + 2t_p d_p \sum \sigma_p(\varepsilon_{p,j}) \\ &+ \sum A_{s,k} \sigma_s(\varepsilon_{s,k}) = 0 \end{aligned} \quad (6)$$

$$\begin{aligned} \sum M &= bd_c \sum \sigma_c(\varepsilon_{c,i}) y_{c,i} + 2t_p d_p \sum \sigma_p(\varepsilon_{p,j}) y_{p,j} \\ &+ \sum A_{s,k} \sigma_s(\varepsilon_{s,k}) y_{s,k} = M \end{aligned} \quad (7)$$

where  $\sigma_c(\varepsilon_c)$ ,  $\sigma_p(\varepsilon_p)$ , and  $\sigma_s(\varepsilon_s)$  are the stress-strain relationships of concrete, steel plates and rebars respectively. Therefore, by employing the strain and curvature factors ( $\alpha_\varepsilon$  and  $\alpha_\varphi$ ), a modified moment-curvature analysis can be conducted for a BSP section with a minor modification to the conventional moment-curvature analysis of a RC section.

However, unlike the effects of the longitudinal partial interaction, which have been studied comprehensively (Newmark *et al.* 1951, Siu 2009), limited studies have been undertaken to investigate the influence of the transverse partial interaction. Oehlers *et al.* (Oehlers *et al.* 1997) established the relationship between the degree of transverse partial interaction and the properties of anchor bolts, in which the uniform shear distribution assumption on

the steel-concrete interface was employed. Based on this model, Nguyen *et al.* (Nguyen *et al.* 2001) derived the relationship between longitudinal and transverse partial interactions. Zhu *et al.* (Zhu *et al.* 2007) found that the translational and rotational partial interactions of the shear connectors would weaken the load-carrying capacity of the steel plates. Su and Siu (Siu and Su 2007, Siu and Su 2011) proposed a procedure to predict transverse slip, despite the fact that the assumption of a linear transverse slip profile has yet to be verified by extensive experimental results. Li *et al.* (Li *et al.* 2013) conducted an experimental study to investigate the transverse slip profile and shear transfer profile along the beam span for four-point-bent BSP beams with different strengthening details. Su *et al.* (Su *et al.* 2013) conducted a numerical study to investigate the variation of shear transfer due to the changes in beam geometry, strengthening arrangements and loading conditions. Kolsek *et al.* (Kolsek *et al.* 2013) proposed a new mathematical model and analytical solution for the analysis of the stress-strain state of a linear elastic BSP beams; an important novelty of the model to mention was that both longitudinal and transversal interactions in BSP beams were considered. However, the solution was based on several ordinary differential equations and an explicit solution that can be used conveniently by engineers was not provided.

Due to the complicated nature of transverse partial interaction, it is difficult to obtain a closed-form explicit analytical solution for the transverse slip and shear transfer. In this study, a piecewise linear model is proposed to yield explicit equations for estimating the shape of the shear transfer of BSP beams, based on the simplified shear transfer profiles derived from a previous numerical study (Su *et al.* 2013). Then the magnitude of the piecewise linear shear transfer profile is determined by considering the displacement compatibility and force boundary conditions. The experimental results (Li *et al.* 2013) of four BSP beams with different bolt-plate arrangements subject to four-point bending were employed to verify the proposed model. Simplified design formulae for calculating the maximum transverse slips and bolt shear forces, as well as the minimum curvature factors under several basic load cases were also developed to facilitate the design of BSP beams, those under more complicated loading conditions can be solved by employing the force superposition principle. A worked example was also provided to illustrate the feasibility of the proposed design formulae.

## 2. Theoretical model

When a simply supported BSP beam is subjected to an applied point load at the midspan as shown in Fig. 2(a), the RC beam bends down with a maximum curvature at the midspan, thus imposes a downward transverse shear force on the steel plates through the shear transfer of the bolt connection. Since the steel plates are not supported by external supports, they transfer the transverse shear force back to the RC beam away from the loading region to achieve equilibrium of vertical forces. Therefore, the

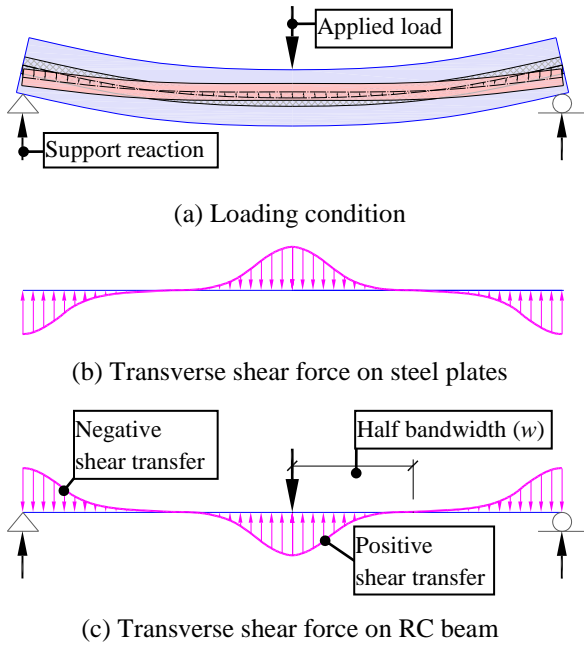


Fig. 2 Shear transfer profiles of a BSP beam under a point load at the midspan

transverse forces on the steel plates are as illustrated in Fig. 2(b), and those on the RC beam are as shown in Fig. 2(c), which include the positive shear transfer at the midspan, the negative shear transfer near the supports, and the external applied load and the support reactions.

### 2.1 Simplified piecewise linear shear transfer model

The distribution of the transverse shear transfer is very difficult to derive by an analytical analysis. However, it can be obtained conveniently by employing a nonlinear finite element analysis (FEA) (Su *et al.* 2013). The entire shear transfer profiles of BSP beams under different load cases, which were derived from FEA numerical study, were shown in Fig. 3.

Fig. 3(a) shows the same load case as that in Fig. 2, where the positive and the negative shear transfers are found to be localised in a small region. Fig. 3(b) shows a load case in which the point load is closer to the right support, where the shear transfer increases, while that at the other support decreases to achieve force equilibrium. Fig. 3(c) presents a load case in which two widely separated point loads are imposed on the BSP beam simultaneously. The interaction between the two shear transfer regions can be neglected. Fig. 3(d) shows the last load case, in which the two point loads are close to each other. The two shear transfer profiles are found to overlap and interact with each other, and the positive shear transfer in the overlapping region accumulates due to the force superposition effects.

It is worth noting that each of these profile curves can be simplified as a piecewise linear polyline. Therefore, a simplified piecewise linear model may be developed for determining the shear transfer profile in BSP beams. The basic assumptions of the proposed model are as follows:

(1) The plane section assumption and the small

deformation flexural theory, i.e., the Bernoulli hypothesis, is adopted for both the RC beam and the steel plates.

(2) The bond-slip effect of both tensile and compressive reinforcement is ignored, i.e., the strain in the rebars is the same as that in the surrounding concrete.

(3) The tensile strength of concrete is ignored; the compressive stress of concrete, the tensile and compressive stresses in reinforcing steel and plate steel can be computed by any proper stress-strain relations.

(4) The shear force-slip relationship of bolt connection is linearly elastic

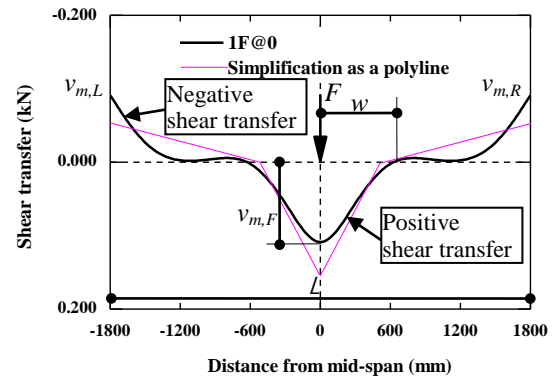
$$S_r = v_m / k_m \quad (8)$$

where  $v_m$  is the transverse shear transfer,  $S_r$  is the transverse slip, and  $k_m$  is the stiffness of bolt connection.

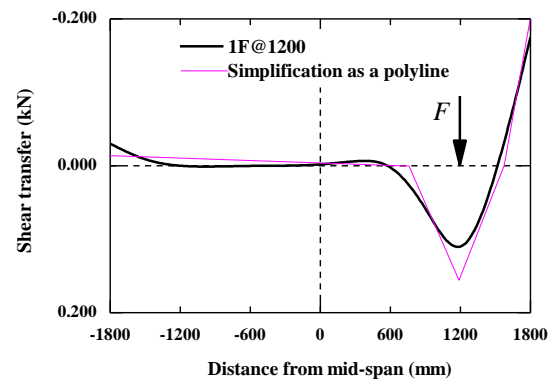
(5) The parabolic positive shear transfer distribution at the loading point is simplified as a triangular profile composed of piecewise straight lines, as shown in Fig. 3(a)-(c).

(6) When adjacent loads are close to each other, the shear transfer in the overlap region is computed based on superposition principle, as shown in Fig. 3(d).

(7) The negative shear transfer distribution near the support is also simplified as a linear profile.

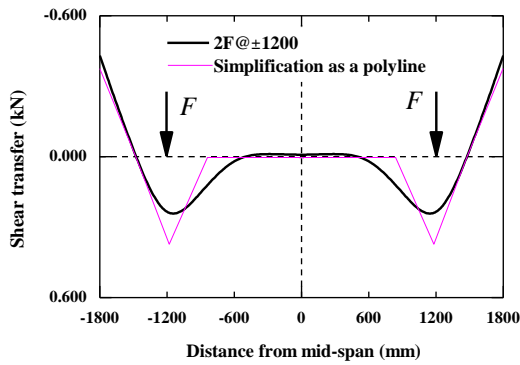


(a) Under a point load at the midspan

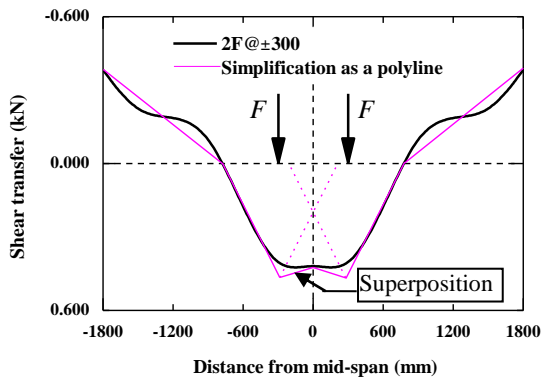


(b) Under a point load close to the support

Fig. 3 Shear transfer profiles of a BSP beam under different load conditions



(c) Under two point loads close to the supports



(d) Under two point loads close to the midspan

Fig. 3 Continued

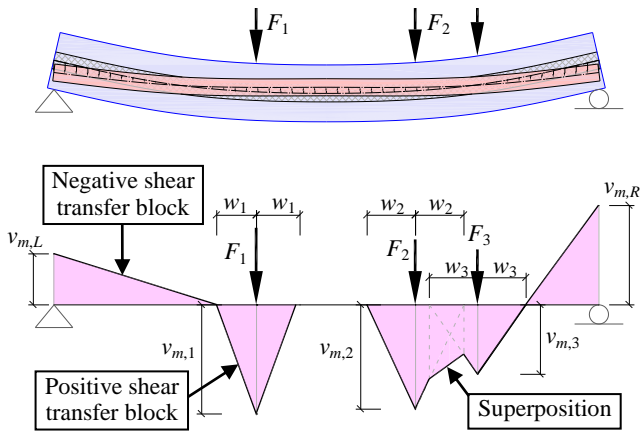


Fig. 4 The piecewise linear profile model for transverse slip and shear transfer in BSP beams

Based on the above assumptions, the proposed piecewise linear shear transfer model for a simply supported BSP beam under arbitrary point loads is illustrated in Fig. 4. It can be observed that each applied point load ( $F_i$ ) acting on the beam span induces an isosceles-triangle-shaped stress block for the positive shear transfer, with a maximum magnitude of  $v_{m,i}$  and a width of  $2w_i$ . The support reactions induce right-triangle-shaped stress blocks for negative shear

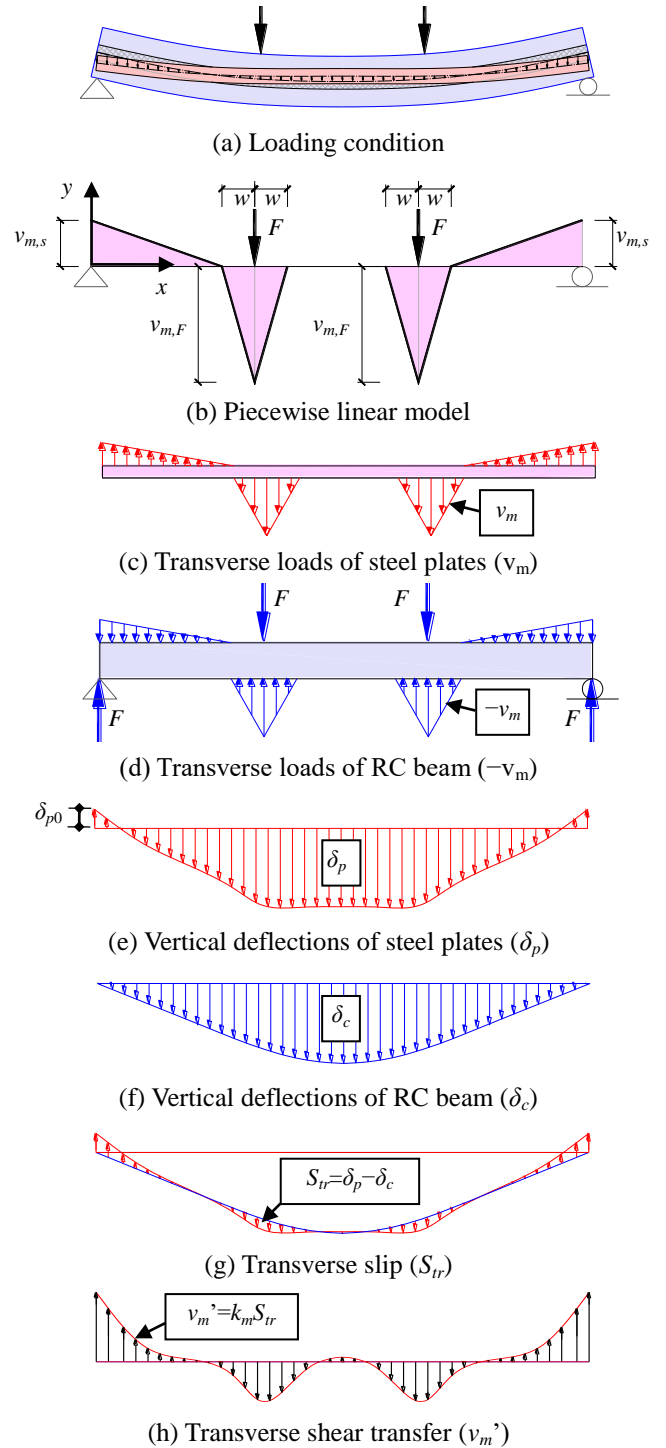


Fig. 5 Linear transverse shear transfer model for a BSP beam under four-point bending

transfers, with a peak value of  $v_{m,L}$  for the left support and  $v_{m,R}$  for the right support.

### 2.2 Transverse shear transfer in a BSP beam under four pointing bending

The shear transfer profile of a simply supported BSP beam under four-point bending (as shown in Fig. 5) is expressed as a piecewise linear function controlled by



$$\xi_F = 132 \cdot (1 - 3\xi_w) / \left[ (1 + 1/\beta_p) \left( \begin{aligned} &52\xi_w^2 - 141\xi_w^3 - 693\xi_w^4 \\ &+ 2484\xi_w^5 - 972\xi_w^6 - 1944\xi_w^7 \\ &- 34992\xi_w^8 L^4 \beta_m^{-1} \end{aligned} \right) \right] \quad (15)$$

Solving Eq. (14) gives the unknown constant  $\xi_w$  and substituting Eq. (14) into Eq. (15) gives the unknown  $\xi_F$ .

However, it is evident that Eq. (14) is not convenient for strengthening design because computer software is needed to solve this 6th-order polynomial equation. On the other hand, by implementing the numerical results (Su *et al.* 2013) of  $\xi_w$  for a BSP beam under four point bending as following

$$\xi_w = \begin{cases} 0.139, & D_p \leq D_c/3 \\ 0.167, & D_p \geq D_c/2 \end{cases} \quad (16)$$

where  $D_c$  and  $D_p$  is thickness of the RC beam and the steel plates respectively. The maximum transverse slips  $S_{tr,max}$  at the supports (i.e.,  $x=0$ ) and the loading points (i.e.,  $x=L/3$ ), and the minimum curvature factor  $\alpha_{\phi,min}$  at the midspan (i.e.,  $x=L/2$ ) can be computed as follows

$$S_{tr,max}|_{x=0} = \begin{cases} \frac{FL^3}{(EI)_c [0.032L^4 \beta_m (1 + \beta_p^{-1}) - 44.4]}, & D_p \leq D_c/3 \\ \frac{FL^3}{(EI)_c [0.025L^4 \beta_m (1 + \beta_p^{-1}) - 44.4]}, & D_p \geq D_c/2 \end{cases} \quad (17)$$

$$S_{tr,max}|_{x=L/3} = \begin{cases} 0.7 \times S_{tr,max}|_{x=0}, & D_p \leq D_c/3 \\ 0.5 \times S_{tr,max}|_{x=0}, & D_p \geq D_c/2 \end{cases} \quad (18)$$

$$\alpha_{\phi,min}|_{x=L/2} = \begin{cases} \frac{1}{(1.8 + 0.8\beta_p - 2500\beta_p L^4 \beta_m^{-1})}, & D_p \leq \frac{D_c}{3} \\ \frac{1}{(3.6 + 2.7\beta_p - 6500\beta_p L^4 \beta_m^{-1})}, & D_p \geq \frac{D_c}{2} \end{cases} \quad (19)$$

### 2.3 Transverse shear transfer in a BSP beam under other loading conditions

For a BSP beam under symmetrical three-point bending, by employing the aforementioned strategy, the design formulae can also be derived similarly as follows

$$S_{tr,max}|_{x=0} = \begin{cases} \frac{FL^3}{(EI)_c [0.114L^4 \beta_m (1 + \beta_p^{-1}) - 77.0]}, & D_p \leq D_c/3 \\ \frac{FL^3}{(EI)_c [0.092L^4 \beta_m (1 + \beta_p^{-1}) - 77.0]}, & D_p \geq D_c/2 \end{cases} \quad (20)$$

$$S_{tr,max}|_{x=L/2} = \begin{cases} 2.2 \times S_{tr,max}|_{x=0}, & D_p \leq D_c/3 \\ 1.0 \times S_{tr,max}|_{x=0}, & D_p \geq D_c/2 \end{cases} \quad (21)$$

$$\alpha_{\phi,min}|_{x=L/2} = \begin{cases} \frac{1}{0.93 - 0.07\beta_p - 625\beta_p L^4 \beta_m^{-1}}, & D_p \leq D_c/3 \\ \frac{1}{2.21 + 1.21\beta_p - 1840\beta_p L^4 \beta_m^{-1}}, & D_p \geq D_c/2 \end{cases} \quad (1)$$

For a BSP beam under asymmetrical three-point bending (the loading position is  $x_F/L=1/4$ ), the design formulae can also be derived similarly as follows

$$S_{tr,max}|_{x=0} = \begin{cases} \frac{FL^3 [0.0021(1 + \beta_p^{-1})\xi_F - 0.091]}{(EI)_c}, & D_p \leq D_c/3 \\ \frac{FL^3 [0.0015(1 + \beta_p^{-1})\xi_F - 0.091]}{(EI)_c}, & D_p \geq D_c/2 \end{cases} \quad (23)$$

$$S_{tr,max}|_{x=L/4} = \begin{cases} \frac{FL^3 [0.0035(1 + \beta_p^{-1})\xi_F - 0.024]}{(EI)_c}, & D_p \leq D_c/3 \\ \frac{FL^3 [0.0021(1 + \beta_p^{-1})\xi_F - 0.024]}{(EI)_c}, & D_p \geq D_c/2 \end{cases} \quad (24)$$

$$\alpha_{\phi,min}|_{x=L/4} = \begin{cases} \frac{1}{\beta_p (10.8\xi_F^{-1} - 1)}, & D_p \leq D_c/3 \\ \frac{1}{\beta_p (8.9\xi_F^{-1} - 1)}, & D_p \geq D_c/2 \end{cases} \quad (25)$$

$$\xi_F = \begin{cases} \frac{1}{0.022(1 + \beta_p^{-1}) - 182L^4 \beta_m^{-1}}, & D_p \leq D_c/3 \\ \frac{1}{0.168(1 + \beta_p^{-1}) - 216L^4 \beta_m^{-1}}, & D_p \geq D_c/2 \end{cases} \quad (26)$$

According to the superposition principle, the internal reaction of a structural member under a uniformly distributed load (UDL) can be simulated by that under a group of uniformly spaced point loads. Therefore, the shear transfer profile of a BSP beam under UDL can be estimated by that under several uniformly spaced point loads. For brevity, instead of simulating the UDL by many point loads, the shear transfer profile under UDL is approximated by that under three point loads with some modification (see Fig. 6): the shear transfer between adjacent point loads is simulated by connecting the maximum shear transfers at the loading points using piecewise lines. Then by employing the same aforementioned strategy, the design formulae can also be derived similarly as follows

$$S_{tr,max}|_{x=0} = \frac{\xi_S}{L^4 \beta_m} \cdot \frac{qL^4}{(EI)_c} \quad (27)$$

$$S_{tr,max}|_{x=L/2} = \frac{\xi_F}{L^4 \beta_m} \cdot \frac{qL^4}{\beta_m (EI)_c} \quad (28)$$

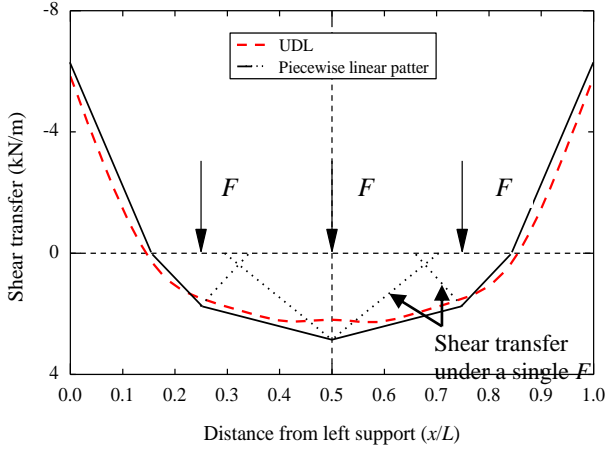


Fig. 6 Shear transfer profile model for a BSP beam under UDL

$$\alpha_{\varphi, \min} \Big|_{x=L/2} = \begin{cases} \frac{0.72L^4\beta_m [5400\beta_p + L^4\beta_m(\beta_p + 1)]}{L^8\beta_m^2(\beta_p + 1)(\beta_p + 0.65) + 20100\beta_p [L^4\beta_m(\beta_p + 0.9) - 5000\beta_p]}, & D_p \leq \frac{D_c}{3} \\ \frac{0.63L^4\beta_m [10300\beta_p + L^4\beta_m(\beta_p + 1)]}{L^8\beta_m^2(\beta_p + 1)(\beta_p + 0.65) + 14600\beta_p [L^4\beta_m(\beta_p + 0.8) - 5500\beta_p]}, & D_p \geq \frac{D_c}{2} \end{cases} \quad (29)$$

$$\xi_S = \begin{cases} \frac{20L^4\beta_m\beta_p [29300\beta_p + L^4\beta_m(\beta_p + 1)]}{C}, & D_p \leq D_c/3 \\ \frac{25L^4\beta_m\beta_p [21100\beta_p + L^4\beta_m(\beta_p + 1)]}{C}, & D_p \geq D_c/2 \end{cases} \quad (30)$$

$$\xi_F = \begin{cases} \frac{1.6L^4\beta_m\beta_p [254900\beta_p - L^4\beta_m(\beta_p + 1)]}{C}, & D_p \leq D_c/3 \\ \frac{3.6L^4\beta_m\beta_p [72300\beta_p + L^4\beta_m(\beta_p + 1)]}{C}, & D_p \geq D_c/2 \end{cases} \quad (31)$$

$$C = \begin{cases} L^8\beta_m^2(\beta_p + 1)^2 + 28200\beta_p [L^4\beta_m(\beta_p + 1) - 5500\beta_p], & D_p \leq \frac{D_c}{3} \\ L^8\beta_m^2(\beta_p + 1)^2 + 16900\beta_p [L^4\beta_m(\beta_p + 1) - 7200\beta_p], & D_p \geq \frac{D_c}{2} \end{cases} \quad (32)$$

The comparison between the results of a BSP beam under a UDL derived from the simplified model and the numerical study (Su *et al.* 2013) is shown in Fig. 6, and good agreement can be found.

By utilising Eqs. (17)-(32), the distribution of the transverse shear transfer of a BSP beam under the basic loading conditions can be determined. Furthermore, by employing the superposition principle, the transverse shear transfer under other complicated loading condition can also be determined.

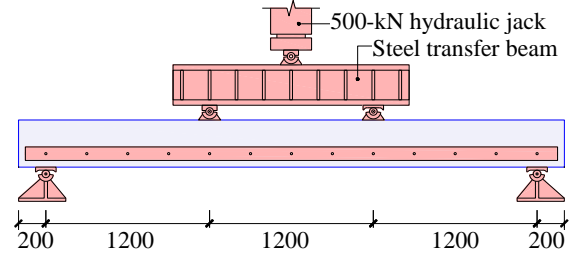
Eqs. (17)-(32) also indicate that the maximum transverse slip  $S_{tr, \max}$  is proportional to the magnitude of the external loads ( $F$  or  $q$ ), while the minimum curvature factor  $\alpha_{\varphi, \min}$  is independent of the magnitude of external loads.

#### 2.4 Verification by experimental results

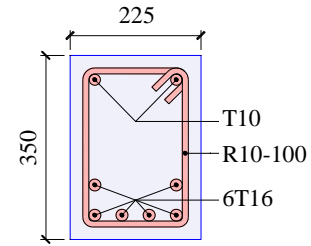
In a previous experimental study (Li *et al.* 2013), the transverse shear transfer profiles of four BSP beams under four point bending were investigated, as shown in Fig. 7. Steel plates with a thickness of 6 mm and two different depths of 100 mm and 250 mm were bolted to the beam's

sides by one or two rows of anchor bolts with a longitudinal spacing of 300 mm or 450 mm to yield distinct strengthening effects. To prevent the plate from buckling, which might otherwise occur in the compressive regions, buckling restraint devices were added. The transverse slips between the steel plates and the RC beams along the beam span were measured by linear variable differential transducers (LVDTs). The shear transfer profiles were then computed based on the measured transverse slips and the load-slip relationship of anchor bolts.

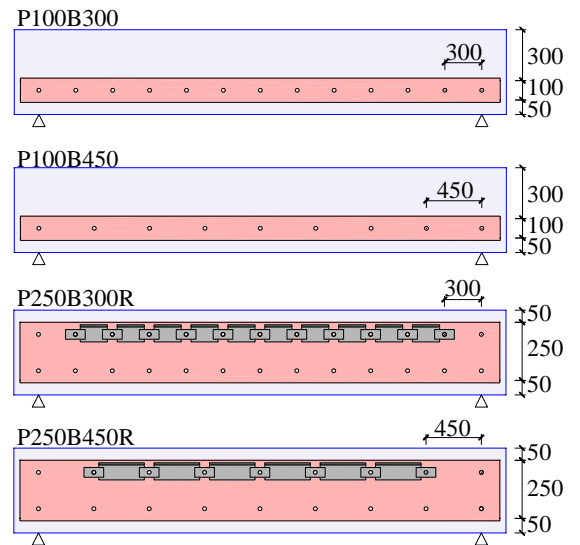
The comparison between the experimental and theoretical transverse shear transfer profiles for all the specimens at the load level  $F/F_p=0.5$  is shown in Fig. 8. These figures indicate that the piecewise linear model is generally capable of predicting the behaviour of transverse shear transfer in BSP beams of different beam geometries.



(a) Test set-up

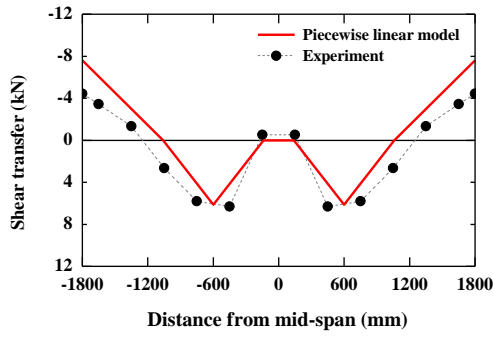


(b) Cross-section

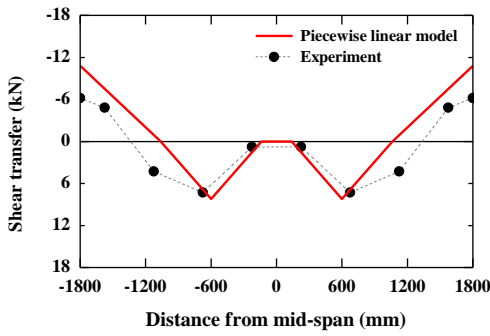


(c) Strengthening arrangements

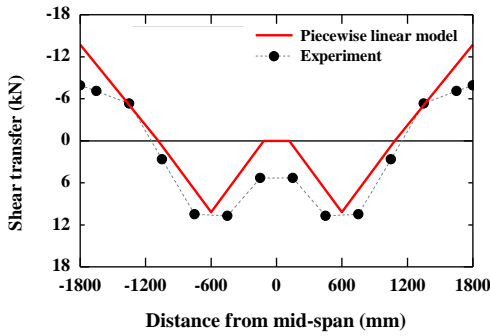
Fig. 7 Specimen details (dimensions in mm)



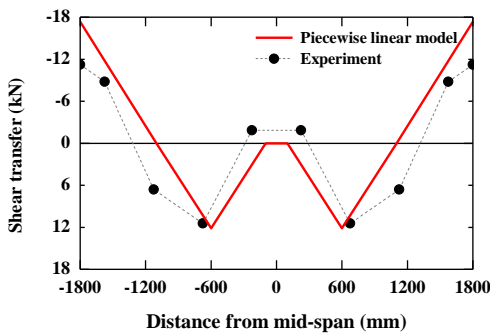
(a) P100B300



(b) P100B450



(c) P250B300R



(d) P250B450R

Fig. 8 Comparison of experimental and theoretical shear transfer profiles at load level  $F/F_p=0.5$

The comparison between the experimental and theoretical transverse shear transfer at the supports and near the loading points for all the specimens are tabulated in Table 1. It is evident that the theoretical model can predict

Table 1 Comparison between the experimental and theoretical transverse shear transfer

	P100B300	P100B450	P250B300R	P250B450R	
$S_s^*$	Experimental	4.3	6.1	7.9	11.2
	Theoretical	7.6	10.8	13.7	17.4
	Error	43.40%	43.50%	42.30%	35.60%
	Average error	41.20%			
$S_p$	Experimental	5.6	7.9	11.1	11.6
	Theoretical	6.1	8.2	10.2	12.1
	Error	8.20%	3.70%	8.80%	4.10%
	Average error	6.20%			

\* $S_s$ : shear transfer in at the support;  $S_p$ : shear transfer near the loading point

the transverse shear transfer near the loading point very well, the maximum discrepancy is 8.8% and the average error is 6.2%. However, it failed to predict the transverse shear transfer in at the support, the maximum discrepancy is 43.5% and average is 41.2%. This is because in our theoretical model, a linear shear force-slip relation is assumed for the bolt connection, and the influence of the longitudinal shear transfer is ignored. However, for the specimens in the experimental study, the actual bolt shear deformation is not linear and the longitudinal and transverse shear transfers interact with each other. According to the experimental investigation (Li *et al.* 2013), the longitudinal slips at the support were about 8 times of the transverse slips, thus the bolt connect at this location was no longer linear and the shear stiffness  $k_m$  degraded considerably. Therefore, to yield a more accurate solution for the shear transfer at the supports, this degradation in  $k_m$  should be taken into account.

### 3. Worked example

Consider a simply supported BSP beam under four-point bending as shown in Fig. 9. The clear span is 7200 mm and the cross section is 350×700 mm. Compression reinforcement of 3T20 and tension reinforcement of 4T25 are employed. Two steel plates of 6×400 mm are bolted to the side faces of the beam by 2 rows of anchor bolts at a horizontal spacing of 150 mm. The material properties are as follows

$$\begin{cases} f_c = 20 \text{ MPa} , E_c = 23 \text{ GPa} \\ f_y = 400 \text{ MPa} , E_s = 200 \text{ GPa} \\ f_{yp} = 355 \text{ MPa} , E_p = 210 \text{ GPa} \\ R_{by} = 28.3 \text{ kN} , S_{by} = 1.5 \text{ mm} \end{cases} \quad (33)$$

The flexural stiffness of the cracked RC beam section, the flexural stiffness of the steel plates, and the stiffness of the bolt connection, thus the plate-RC and bolt-RC stiffness ratio ( $\beta_p$  and  $\beta_m$ ) can be computed based on the beam geometry and the material properties, which are given by

$$\begin{cases} (EI)_c = 6.69 \times 10^{13} \text{ N} \cdot \text{mm}^2 \\ (EI)_p = 1.34 \times 10^{13} \text{ N} \cdot \text{mm}^2 \\ k_m = 251 \text{ N/mm}^2 \end{cases} \quad (34)$$

$$\begin{cases} \beta_p = \frac{1.34 \times 10^{13}}{6.69 \times 10^{13}} = 0.201 \\ \beta_m = \frac{251}{6.69 \times 10^{13}} = 3.76 \times 10^{-12} \text{ mm}^{-4} \end{cases} \quad (35)$$

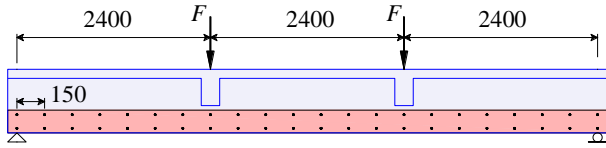
By substituting Eq. (35) into Eq. (19), the minimum curvature factor ( $\alpha_{\varphi, \min}$ ) at the loading points (i.e.,  $x=L/3$ ) can be computed as

$$\alpha_{\varphi, \min} = \frac{1}{3.6 + 0.8 \times 0.201 - \frac{2500 \times 0.201}{7200^4 \times 3.76 \times 10^{-12}}} = 0.25 \quad (36)$$

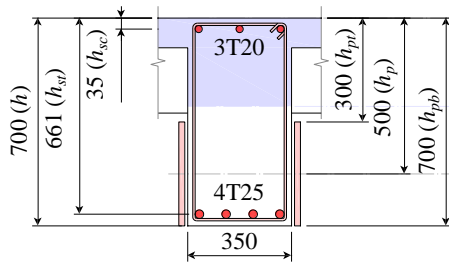
The computation of the minimum strain factor ( $\alpha_{\varepsilon, \min}$ ) can be referred to a previous paper (Su *et al.* 2014). For brevity, only the result is listed as following

$$\alpha_{\varepsilon, \min} = 0.50 \quad (37)$$

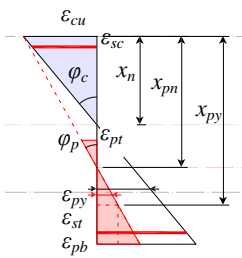
By employing a modified moment-curvature analysis with the consideration of partial interaction as shown in



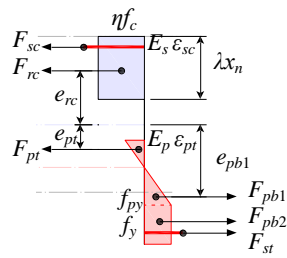
(a) Elevation layout (dimensions in mm)



(b) Cross-section (dimensions in mm)



(c) Strain profile



(d) Stress profile

Fig. 9 An example of the evaluation of transverse partial interaction in a BSP beam

Eqs. (3)-(6), the ultimate flexural strength  $M_u$  can be computed. For illustration purpose, the simplified method as shown in Fig. 9 is employed herein to compute  $M_u$ .

According to Eqs. (3)-(5), the strains of the compressive concrete surface ( $\varepsilon_{cu}$ ), the compressive and tensile rebars ( $\varepsilon_{sc}$  and  $\varepsilon_{st}$ ), and the top and bottom edges of the steel plates ( $\varepsilon_{pt}$  and  $\varepsilon_{pb}$ ) can be expressed in terms of the curvature and the neutral axis depth ( $\varphi_c$  and  $x_n$ ) as follows (see Fig. 9(c))

$$\begin{cases} \varepsilon_{cu} = \varphi_c x_n \\ \varepsilon_{sc} = \varphi_c (x_n - h_{sc}) = \varphi_c (x_n - 35) \\ \varepsilon_{st} = \varphi_c (h_{st} - x_n) = \varphi_c (661 - x_n) \\ \varepsilon_{pt} = \alpha_{\varphi} \varphi_c (h_p - h_{pt}) - \alpha_{\varepsilon} \varphi_c (h_p - x_n) \\ \quad = 50 \varphi_c - 0.50 \varphi_c (500 - x_n) \\ \varepsilon_{pb} = \alpha_{\varphi} \varphi_c (h_{pb} - h_p) + \alpha_{\varepsilon} \varphi_c (h_p - x_n) \\ \quad = 50 \varphi_c + 0.50 \varphi_c (500 - x_n) \end{cases} \quad (38)$$

Thus the axial forces of the compressive concrete ( $N_{rc}$ ), the compressive and tensile rebars ( $N_{sc}$  and  $N_{st}$ ), and the compressive, the top and bottom tensile parts of steel plates ( $N_{pt}$  and  $N_{pb1}$  and  $N_{pb2}$ ), along with their separations from the RC neutral axis level, can be expressed as follows (see Fig. 9(d))

$$\begin{cases} N_{rc} = \eta f_c b \lambda x_n = 1.0 \times 20 \times 350 \times 0.8 \times x_n \\ \quad = 5.60 \times 10^3 x_n \\ N_{sc} = f_y A_{sc} = 400 \times (3 \times \pi \times 20^2 / 4) \\ \quad = 3.77 \times 10^5 \\ N_{st} = -f_y A_{st} = -400 \times (5 \times \pi \times 25^2 / 4) \\ \quad = -7.85 \times 10^5 \\ N_{pt} = \frac{1}{2} E_p \varepsilon_{pt} (x_{pn} - h_{pt}) \cdot 2t_p \\ \quad = -3.53 \times 10^6 + 4.41 \times 10^3 x_n + 7.06 \times 10^8 / x_n \\ N_{pb1} = -\frac{1}{2} f_{py} (x_{py} - x_{pn}) \cdot 2t_p \\ \quad = -4.14 \times 10^3 x_n \\ N_{pb2} = -f_{py} (h_{pb} - x_{py}) \cdot 2t_p \\ \quad = -5.11 \times 10^6 + 1.68 \times 10^3 x_n \end{cases} \quad (39)$$

$$\begin{cases} e_{rc} = x_n - \frac{1}{2} \lambda x_n = x_n - \frac{1}{2} \times 0.8 x_n = 0.6 x_n \\ e_{sc} = x_n - h_{sc} = x_n - 35 \\ e_{st} = -(h_{st} - x_n) = x_n - 661 \\ e_{pt} = -\left[ h_{pt} + \frac{1}{3} (x_{pn} - h_{pt}) - x_n \right] = -33 + 0.33 x_n \\ e_{pb1} = -\left[ x_{py} - \frac{1}{3} (x_{py} - x_{pn}) - x_n \right] = 500 - 2.30 x_n \\ e_{pb2} = -\left[ h_{pb} - \frac{1}{2} (h_{pb} - x_{py}) - x_n \right] = -100 - 0.97 x_n \end{cases} \quad (40)$$

where  $x_{pn}$  is the neutral axis level of the steel plates and  $x_{py}$  is the yielding level of the steel plates, which can be easily computed by setting the plate strains to be zero and the yielding strain  $\varepsilon_{py}$  of steel plates as follows

$$\begin{cases} \varepsilon_{p, x_{pn}} = \alpha_\phi \varphi_c (x_{pn} - h_p) + \alpha_\varepsilon \varphi_c (h_p - x_n) = 0 \\ \Rightarrow x_{pn} = 2.00x_n - 500 \\ \varepsilon_{p, x_{py}} = \alpha_\phi \varphi_c (x_{py} - h_p) + \alpha_\varepsilon \varphi_c (h_p - x_n) = \varepsilon_{py} \\ \Rightarrow x_{py} = 3.94x_n - 500 \end{cases} \quad (41)$$

$$\begin{cases} \frac{M_{u,FI}}{M_u} - 1 = 5.5\% \\ \frac{M_{u,FI} - M_{u,0}}{M_u - M_{u,0}} - 1 = 11.2\% \end{cases} \quad (48)$$

For a flexural beam, the resultant axial force is zero, thus

$$\begin{aligned} N_u &= N_{rc} + N_{sc} + N_{st} + N_{pt} + N_{pb1} + N_{pb2} \\ &= -9.05 \times 10^6 + 2.27 \times 10^4 x_n + 7.06 \times 10^8 / x_n \\ &= 0 \end{aligned} \quad (42)$$

Solving this quadratic equation yield the RC neutral axis level as

$$x_n = 293 \text{ mm} \quad (43)$$

By substituting Eq. (42) back into Eqs. (39)-(40), thus the ultimate flexural strength  $M_u$  can be yielded as

$$\begin{aligned} M_u &= N_{rc} e_{rc} + N_{sc} e_{sc} + N_{st} e_{st} + N_{pt} e_{pt} + N_{pb1} e_{pb1} + N_{pb2} e_{pb2} \\ &= 1640 \times 0.176 + 377 \times 0.258 + 785 \times 0.368 \\ &\quad - 173 \times 0.064 + 1212 \times 0.172 + 192 \times 0.385 \\ &= 968 \text{ kN} \cdot \text{m} \end{aligned} \quad (44)$$

The negative sign in  $N_{pt}$  indicates the steel plates are under tensile stress in the entire section. It is also worth noting that  $x_n$  in Eq. (43) should be substituted into Eq. (38) to check the yielding state of the rebars and steel plates, and subsequent modification might be needed for Eqs. (39)-(40). Then the peak load  $F_p$  can be computed as

$$F_p = \frac{968}{7.2/3} = 398 \text{ kN} \quad (45)$$

By substituting Eq. (45) into Eq. (17), the maximum transverse slip  $S_{r,max}$ , shear transfer  $v_{m,max}$ , and transverse bolt force  $V_{m,max}$  at the support under the peak load  $F_p$  can be obtained as

$$\begin{cases} S_{r,max}|_{x=0} = \frac{398 \times 10^3 \times 7200^3}{6.69 \times 10^{13} \times [0.025 \times 3.76 \times 10^{-12} \times 7200^4 (1 + 0.201^{-1}) - 44.4]} \\ \quad = 1.5 \text{ mm} \\ v_{m,max}|_{x=0} = k_m S_{r,max}|_{x=0} = 251 \times 1.5 = 377 \text{ N/mm} \\ V_{m,max}|_{x=0} = S_b v_{m,max}|_{x=0} = 150 \times 377 = 56.6 \text{ kN} \end{cases} \quad (46)$$

If full interaction assumption is employed, the ultimate flexural strength ( $M_{u,FI}$ ) can also be obtained by replacing the strain and curvature factors in Eqs. (38) and (41) with  $\alpha_\varepsilon = \alpha_\phi = 1$ . Similarly, the ultimate flexural strength ( $M_{u,0}$ ) of the unstrengthened RC beam can also be computed by replacing these two factors with  $\alpha_\varepsilon = \alpha_\phi = 0$ . For brevity, the calculation is not repeated herein and the result is listed as

$$M_{u,FI} = 1021 \text{ kN} \cdot \text{m} > M_u = 968 \text{ kN} \cdot \text{m} > M_{u,0} = 494 \text{ kN} \cdot \text{m} \quad (47)$$

Thus the loading capacity of the beam would be overestimated by 5.5% and the strengthening effect would be overestimated by 11.2%, if the influence of partial interaction is ignored in analysing the bending performance of BSP beams.

#### 4. Conclusions

In this paper, a theoretical study on the transverse shear transfer in BSP beams was presented. Based on the results of this study, the following conclusions are drawn.

(1) The magnitudes of the transverse slip and transverse shear transfer were found to be controlled by the magnitude of the applied load. However, the curvature factor, i.e., the degree of the transverse partial interaction, was controlled by the stiffness of the RC beam, the steel plates and the connection medium and not by the magnitude of applied loads.

(2) For BSP beams under four-point bending, the proposed piecewise linear shear transfer model could generally predict the distribution profile of the transverse shear transfer. It could predict the transverse shear transfers near the loading point, but failed for those at the supports.

(3) The proposed design formulae of the maximum transverse slip, the maximum transverse bolt shear force, and the minimum curvature factor, can be used for the strengthening design of BSP beams.

#### Acknowledgements

The research described in this paper received financial support from the Research Grants Council of the Hong Kong SAR (Project No. HKU7151/10E) and from The University of Hong Kong of the small project funding as well as technical support from the HILTI Corporation, all of which are gratefully acknowledged.

#### References

- Adhikary, B.B., Mutsuyoshi, H. and Sano, M. (2000), "Shear strengthening of reinforced concrete beams using steel plates bonded on beam web: experiments and analysis", *Constr. Build. Mater.*, **14**(5), 237-244.
- Ahmed, M., Oehlers, D. and Bradford, M. (2000), "Retrofitting reinforced concrete beams by bolting steel plates to their sides. Part 1: Behaviour and experiments", *Struct. Eng. Mech.*, **10**(3), 211-226.
- Anil, O., Belgin, C.M. and Kara, M.E. (2010), "Experimental investigation on CFRP-to-concrete bonded joints across crack", *Struct. Eng. Mech.*, **35**(1), 1-18.
- Johnson, R.P. and Molenstra, N. (1991), "Partial shear connection in composite beams for buildings", *ICE Proceedings*, **91**(4),

679-704.

- Kolsek, J., Hozjan, T., Saje, M. and Planinc, I. (2013), "Analytical solution of linear elastic beams cracked in flexure and strengthened with side plates", *J. Compos. Mater.*, **47**(22), 2847-2864.
- Li, L.Z., Lo, S.H. and Su, R.K.L. (2013), "Experimental Study of Moderately Reinforced Concrete Beams Strengthened with Bolted-Side Steel Plates", *Adv. Struct. Eng.*, **16**(3), 499-516.
- Newmark, N.M., Siess, C.P. and Viest, I.M. (1951), "Tests and analysis of composite beams with incomplete interaction", *Proc. Soc. Exp. Stress Anal.*, **9**(1), 75-92.
- Nguyen, N.T., Oehlers, D.J. and Bradford, M.A. (2001), "An analytical model for reinforced concrete beams with bolted side plates accounting for longitudinal and transverse partial interaction", *Int. J. Solids Struct.*, **38**(38), 6985-6996.
- Oehlers, D., Ahmed, M., Nguyen, N. and Bradford, M. (2000), "Retrofitting reinforced concrete beams by bolting steel plates to their sides. Part 2: Transverse interaction and rigid plastic design", *Struct. Eng. Mech.*, **10**(3), 227-243.
- Oehlers, D.J., Nguyen, N.T., Ahmed, M. and Bradford, M.A. (1997), "Transverse and longitudinal partial interaction in composite bolted side-plated reinforced-concrete beams", *Struct. Eng. Mech.*, **5**(5), 553-563.
- Siu, W.H. (2009), "Flexural strengthening of reinforced concrete beams by bolted side plates", Ph.D.Dissertation, the University of Hong Kong, Pokfulam Road, Hong Kong.
- Siu, W.H. and Su, R.K.L. (2010), "Effects of plastic hinges on partial interaction behaviour of bolted side-plated beams", *J. Constr. Steel Res.*, **66**(5), 622-633.
- Siu, W.H. and Su, R.K.L. (2011), "Analysis of side-plated reinforced concrete beams with partial interaction", *Comput. Concrete*, **8**(1), 71-96.
- Smith, S.T. and Bradford, M.A. (1999), "Local buckling of side-plated reinforced-concrete beams. II: Experimental study", *J. Struct. Eng.*, **125**(6), 635-643.
- Su, R.K.L. and Siu, W.H. (2007), "Nonlinear response of bolt groups under in-plane loading", *Eng. Struct.*, **29**(4), 626-634.
- Su, R.K.L. and Zhu, Y. (2005), "Experimental and numerical studies of external steel plate strengthened reinforced concrete coupling beams", *Eng. Struct.*, **27**(10), 1537-1550.
- Su, R.K.L., Li, L.Z. and Lo, S.H. (2013), "Shear transfer in bolted side-plated reinforced concrete beams", *Eng. Struct.*, **56**, 1372-1383.
- Su, R.K.L., Li, L.Z. and Lo, S.H. (2014), "Longitudinal partial interaction in bolted side-plated reinforced concrete beams", *Adv. Struct. Eng.*, **17**(7), 921-936.
- Subedi, N.K. and Baglin, P.S. (1998), "External plate reinforcement for concrete beams", *J. Struct. Eng.*, **124**(12), 1490-1495.
- Zhu, Y. and Su, R. (2010), "Behavior of strengthened reinforced concrete coupling beams by bolted steel plates, Part 2: Evaluation of theoretical strength", *Struct. Eng. Mech.*, **34**(5), 563-580.
- Zhu, Y., Su, R. and Zhou, F.L. (2007), "Seismic behavior of strengthened reinforced concrete coupling beams by bolted steel plates, Part 1: Experimental study", *Struct. Eng. Mech.*, **27**(2), 149-172.